Research Paper

CXCR5 induces perineural invasion of salivary adenoid cystic carcinoma by inhibiting microRNA-187

Mei Zhang[1], Jia-Shun Wu[1], Hong-Chun Xian[1], Bing-Jun Chen[1], Hao-Fan Wang[1], Xiang-Hua Yu[1], Xin Pang[1], Li Dai[1], Jian Jiang[2], Xin-Hua Liang[1], Ya-Ling Tang[1]

[1]State Key Laboratory of Oral Diseases & National Clinical Research Center for Oral Diseases, West China Hospital of Stomatology (Sichuan University), Chengdu 610041, China
[2]Department of Head and Neck Surgery, Sichuan Cancer Hospital, Sichuan Cancer Center, School of Medicine, University of Electronic Science and Technology of China, Chengdu, Sichuan, China

Correspondence to: Xin-Hua Liang, Ya-Ling Tang; **email:** lxh88866@scu.edu.cn, tangyaling@scu.edu.cn
Keywords: salivary adenoid cystic carcinoma (SACC), CXCR5, perineural invasion (PNI), microRNAs (miRNAs), Schwann cells
Received: December 3, 2020 **Accepted:** May 11, 2021 **Published:** June 10, 2021

ABSTRACT

CXCR5 played critical roles in tumorigenesis and metastasis. Nevertheless, little was known about the involvement of CXCR5 in perineural invasion (PNI) of salivary adenoid cystic carcinoma (SACC). Here, we confirmed upregulation of CXCR5 in SACC specimens and cells and identified that CXCR5 exhibited a significant positive correlation with PNI. Functionally, knockdown of CXCR5 suppressed SACC cells migration, invasion and PNI ability, whereas CXCR5 overexpression displayed the opposite effects. Moreover, CXCR5 downregulated microRNA (miR)-187, which could competitively sponge S100A4. The PNI-inhibitory effect of CXCR5 knockdown or miR-187 overexpression could be reversed by elevated expression of S100A4. Conjointly, our data revealed that CXCR5 facilitated PNI through downregulating miR-187 to disinhibit S100A4 expression in SACC.

INTRODUCTION

Salivary adenoid cystic carcinoma (SACC) belongs to malignant epithelial tumor derived from the salivary gland, accounting for about 28% of salivary gland malignancies [1–3]. Despite the progress in surgical resection combination with radiotherapy and/or chemotherapy for SACC, more than 30% of the SACC patients still experience local recurrence and hematogenous spread to distant organs after primary treatments [4–7]. One of the pivotal factors affecting local recurrence or distant metastasis of SACC is perineural invasion (PNI), which refers to tumor cells encroaching along nerves. PNI can hinder curative resection and is predicted to reduce survival rate [8–10]. Thus, it is necessary to elucidate the concrete mechanism driving PNI, which may guide us with a better management of SACC.

The chemokine receptor CXCR5, pertaining to G-protein coupled receptors (GPCR) superfamily, could promote lymphocyte migration and evoke inflammatory responses [11, 12]. Increasing evidence revealed that CXCR5 was highly expressed in many human cancers and was related to occurrence, invasion and metastasis of tumors [13–15]. Recent studies reported that CXCR5 was overexpressed and associated with PNI in colorectal and prostate cancers [16, 17]. Therefore, the role of CXCR5 in PNI of SACC is a burgeoning field of research.

MicroRNAs (miRNAs) are a class of single-stranded non-coding RNAs with a length of 18-25 nucleotides. MiRNAs work via forming RNA-induced silencing complex (RISC) to inhibit mRNAs translation, and they also trigger degradation of target mRNAs through binding to the 3′-UTRs [18, 19]. Moreover, miRNAs emerging as robust players of PNI in perineural niche have aroused wide interest [20]. However, whether miRNAs participate in CXCR5-driven PNI of SACC has not been characterized.

To invade the nerve, tumor cells must rearrange their skeletons and change their morphology to obtain stronger invasiveness. Schwann cells, which have been verified as the main cells of peripheral nerves, are fundamental to the survival and development of nerves and conducive to the maintenance of axons [21, 22]. Substantial evidences suggested that the expression of Schwann cell hallmarks, including S100 calcium binding protein A4 (S100A4), p75 neurotrophin receptor (p75NTR) and glial fibrillary acidic protein (GFAP) were increased considerably in many tumors with PNI, such as melanoma [23], breast cancer [24], prostate cancer [25], colorectal cancer [26]. Therefore, scholars speculated that the differentiation of tumor cells into Schwann-like cells could increase migration and invasion ability of tumor cells. And the Schwann-like differentiation might be one of the mechanisms of PNI occurrence in tumors [27, 28]. In the SACC, Shan et al. found that the expression of S100A4 and GFAP at nerve invasion frontier was dramatically increased [29]. Thereby, we focused on whether CXCR5 could initiate a miRNA mediated network to drive the differentiation of tumor cells into Schwann-like cells in PNI of SACC, promising to identify new biomarkers and offer cancer therapeutic targets.

MATERIALS AND METHODS

Patients and specimen collection

158 patients suffering from SACC and receiving curative surgical resection without chemotherapy, radiotherapy or hormone therapy prior to surgery at West China Hospital of Stomatology, Sichuan University between 2002 and 2007 were enrolled in the cohort with informed consent. The clinicopathological TNM stages were determined according to the International Union Against Cancer TNM classification of malignant tumors [30]. And 20 cases of normal salivary glands adjacent to carcinoma were randomly selected as control. The follow-up information was up-dated on December 31, 2017. The median follow-up of these patients was 83.7 months (range 3.5–140 months). The present study protocol was approved by the Institutional Ethics Committee of West China Medical Center, Sichuan University, China.

Immunohistochemistry (IHC)

All samples were fixed in formaldehyde solution, embedded in paraffin and sectioned for immunohistochemistry (IHC) analysis according to IHC staining procedure. Primary antibodies for CXCR5 (1:250), S100A4 (1:100), p75NTR (1:100), GFAP (1:200) were purchased from Abcam (Cambridge, MA). The slides were observed using DAB and counterstained with hematoxylin. The stained slides were evaluated by two pathologists independently without the knowledge of patients' clinicopathological parameters. The immunoreactive intensity was assigned to − (0), <5%; + (1), 5-25%; ++ (2), 25-50%; +++ (3), >50%, representing negative expression, weakly positive expression, moderately positive expression and strongly positive expression, respectively. − and + mean low expression, and ++ and +++ mean high expression.

Cell line and cell culture

SACC cell lines (SACC-83 and SACC-LM) and nerve cell line microglia BV2 were provided by State Key Laboratory of Oral Diseases & National Clinical Research Center for Oral Diseases, West China Hospital of Stomatology, Sichuan University and maintained in Dulbecco's Modified Eagle's Medium (DMEM) (Gibco, US), supplemented with 10% fetal bovine serum (FBS) (Gibco, US), 50 mg/ml streptomycin and 50 unit/ml penicillin (Gibco, US) at 37°C with 5% CO2 in humidified incubators.

Cell transfection

SiRNA targeting CXCR5, negative control siRNA (Control), negative control miRNA mimic (NC mimic), miR-187 mimic (miR-187), negative control miRNA inhibitor (NC inhibitor) and miR-187 inhibitor were synthesized by GenePharma. CXCR5 and S100A4 were integrated into pcDNA3.1 (Invitrogen, Carlsbad, CA) for overexpression experiments. SACC cells at ~50% confluence were transfected with Lipofectamine 2000 reagent (Invitrogen, Carlsbad, CA) in conformity with the manufacturer's protocol. Besides, blank group (only transfection reagent) was used as blank control group (Blank). The medium containing Lipofectamine 2000 was changed into RPMI-1640 with 10% FBS after 6 h. The cells were collected for the following experiments after 48 h transfection.

Immunofluorescence staining

SACC cells were seeded on coverslips, incubated for 24 h, fixed with 4% formaldehyde for 15 min, permeabilized with 0.5% Triton X-100 for 10 min and blocked with 10% normal goat serum for 1 h. Then, primary antibodies against CXCR5 were incubated overnight at 4°C. Next day, cells were incubated with fluorescein-conjugated secondary antibodies for 1 h and the nuclei was stained with 4′, 6-diamidino-2-phenylindole (DAPI). Images were captured using a fluorescence microscope (Leica, Germany).

Quantitative real-time PCR (qRT-PCR)

Total RNA was extracted from cells and tissue using TRIzol reagent (Takara, Tokyo, Japan) and the quantity and quality of RNA were measured with the NanoDrop ND-1000 Spectrophotometer (Thermo Scientific Inc., Waltham, MA). Then, RNA was reverse-transcribed into miRNA cDNA and total cDNA respectively using One Step PrimeScript miRNA cDNA Synthesis Kit and SuperScript™ III First-Strand Synthesis Kit, respectively. QRT-PCR was conducted according to the protocol provided by the manufacturer using the PCR primer sequences in Supplementary Table 1. U6 was served as an endogenous control for miRNA, and mRNA were normalized to GAPDH. Each experiment was conducted in triplicate.

Scratch wound healing assay

1.0 μg/ml of anti-human CXCR5 antibody (R&D Systems) was added to 6-well plates after SACC cells were seeded [17]. When SACC cells were at a density of 95%, scratches were created with a 200 μL pipette tip and detached cells were removed with PBS rinsing. And the scratches were observed and photographed at 0 h and 24 h. Percentage of wound closure was statistically analyzed using Image-Pro Plus Analysis software (Media Cybernetics company, Rockville, Maryland).

Transwell invasion assay and co-culture assay

For the Matrigel invasion assays, SACC cells (1×10^5) were seeded into the upper chamber of the Corning Matrigel Invasion insert covered with Matrigel (pore size, 8.0 μm; BD Biosciences) containing 200 μL serum-free medium with 1.0 μg/ml of anti-human CXCR5 antibody. The bottom chamber was filled with 500 μL medium containing 10% FBS. The cells were fixed in 4% paraformaldehyde and then stained with 0.05% crystal violet after 48 h. Cells penetrated the membrane to the bottom of the chamber were counted in five random fields.

To investigate the role of CXCR5 in PNI of SACC, co-culture assay was conducted based on the model previously employed by He et al. [31, 32]. In brief, BV2 cells (1×10^5) were seeded into the 24-well plates. The next day, Boyden Chamber was inserted and SACC cells were seeded into Boyden Chamber covered with Matrigel and treated with 1.0 μg/ml of anti-human CXCR5 antibody. The number of invasive cells penetrating the membrane to the bottom of the chamber was counted after Transwell chamber was incubated for 48 h.

TRITC-phalloidin staining for detecting cytoskeletal reorganization

SACC cells were fixed with 4% paraformaldehyde for 15 min, lysed with 0.2% Triton X-100 for 15 min and blocked with 5% BSA for 20 min. Immediately, cytoskeleton dye TRITC-phalloidin (Sigma) was incubated for 30 min and DAPI was used for nuclei staining. Images were visualized and captured using a fluorescence microscope.

MiRNA microarray

Total RNA of control or si-CXCR5 SACC-LM cells was extracted with the TRIzol reagent (Invitrogen), purified using the NanoPhotometer® spectrophotometer (IMPLEN, CA) and subjected to a miRNA microarray. Data analysis was performed via GeneSpring software (Agilent). For selecting differently expressed genes, absolute value fold change of at least 1.5 and a *p*-value less than 0.05 was used as the cut-off value.

Fluorescent *in situ* hybridization (FISH)

Fish analysis was conducted on paraffin section. Cy3-labeled miR-187 and FISH Kit (RiboBio, Guangzhou, China) were used following the manufacturer's instructions.

Luciferase reporter assay

Wild-type (Wt) and mutated-type (Mut) human S100A4 3′-UTR containing the miR-187 binding site were synthesized and co-transfected with miR-187 mimic or NC mimic into SACC cells. After 48 h of transfection, luciferase activity was determined by Dual-Luciferase Reporter Assay System and normalized to Renilla luciferase in each well.

In vivo PNI model

To determine whether CXCR5 played an essential role in the occurrence of PNI in SACC, 16 athymic nude mice aged 5 weeks were purchased. Under sterile conditions, the mice received groin injection of 2.5×10^6 SACC-LM cells in phosphate buffered saline (PBS). 2 weeks after inoculation, 16 nude mice were randomly allocated into two group, including saline group (n = 8, treatment with saline at 0.1 ml/day) and anti-CXCR5 antibody group (n = 8, treatment with anti-CXCR5 antibody at 1.0 μg/day injected into the tumor site), which referenced and improved previous study about the usage of antibody *in vivo* [33, 34], and receive corresponding treatment for 2 weeks, respectively. Sciatic nerve function, which intervened functional movement of hind limbs in nude mice was monitored

for 2 weeks. Tumor was surgically removed and subsequent experiments were conducted.

Statistical analysis

The expression of CXCR5 in different PNI status and the association between CXCR5 expression and patients' clinicopathologic parameters were analyzed by Wilcoxon test. The relationship between CXCR5 expression and the expression of Schwann cell hallmarks at nerve invasion front was evaluated by Spearman's rank correlation analysis. SPSS software package 21.0 (SPSS, Chicago, IL, USA) was used to conduct the statistical analyses. Differences were considered statistically significant when p value was less than 0.05 and statistical differences among multiple groups were corrected using Bonferroni for multiple testing.

Ethics approval and consent to participate

The use of human tissue samples and clinical data was approved by the Institutional Ethics Committee of the West China Medical Center, Sichuan University, China (WCHSIRB-D-2016-207, WCHSIRB-D-2017-120). The written informed consents were obtained from participants through their signatures. All procedures involving animal were approved by the Subcommittee on Research and Animal Care (SRAC) of Sichuan University (WCHSIRB-D-2016-191).

Availability of data and material

All data generated or analyzed during this study are included in this published article and its supplementary files.

RESULTS

Overexpression of CXCR5 contributes to PNI in SACC samples

Among 158 SACC cases, the incidence of PNI is 48.7% (77/158) via HE staining. The clinicopathologic characteristics of patients were summarized in Table 1. IHC staining showed that CXCR5 was generally expressed in cytoplasm and/or cytomembrane, with 75% (15/20) negative expression and 25% (5/20) weak expression out of 20 cases normal salivary gland (NSG). However, the positive rate of CXCR5 was 81.0% (128/158) in SACC specimens. The expression of CXCR5 in SACC specimens was noticeably higher versus NSG group ($p < 0.0001$) (Figure 1A). CXCR5 expression was significantly associated with patients' tumor site, clinical stage, involvement of surgical margin, local regional recurrence, distant metastasis and histological subtype ($p = 0.038$, $p = 0.017$, $p = 0.04$, $p = 0.008$, $p = 0.001$ and $p = 0.008$, respectively), but not with age, sex, complaint and tumor size (all $p > 0.05$) (Table 1). Subsequently, Kaplan-Meier curve revealed that SACC patients with high CXCR5 expression level had a significantly worse overall survival (OS) than those with lower CXCR5 levels (Figure 1B). Multivariate Cox Regression analysis indicated that the elevated CXCR5 level was an independent prognosticator of OS for SACC patients ($p = 0.003$) (Table 2).

To investigate the role of CXCR5 in the PNI of SACC, CXCR5 expression in different PNI status was assessed, and the result revealed that the expression of CXCR5 was increased in the samples with PNI compared to the no-PNI group ($p = 0.005$). And CXCR5 expression levels displayed an increasing trend from far away from nerve site (Far-nerve group) to nerve invasion frontier (Nerve-front group) in SACC with PNI ($p = 0.001$) (Table 3) (Figure 1A). These data suggested that the occurrence of SACC was correlated to the expression of CXCR5, and the high CXCR5 expression was found to be associated significantly with the presence of PNI in SACC.

CXCR5 promotes migration, invasion and PNI in SACC cells

To further ascertain the relationship of CXCR5 and PNI in SACC, siRNA-mediated knockdown assays were performed. CXCR5 level was significantly inhibited after siRNA treatment in SACC cells by immunofluorescence and qRT-PCR analysis, and representative results in SACC-LM cells were displayed in Figure 2A. We observed that CXCR5 knockdown in SACC cells impeded migration in wound healing assays (Figure 2B) and invasion in Matrigel invasion assays (Figure 2C). Meanwhile, the invasive potential of SACC cells towards nerve cell BV2 was also weakened after CXCR5 silencing (Figure 2D). Similarly, CXCR5 blockage induced by anti-CXCR5 antibody notably inhibited migration, invasion and PNI of SACC cells. Moreover, CXCR5-overexpressing plasmid was transfected in SACC-LM cells (Figure 2E), which markedly contributed to migration, invasion and PNI of SACC-LM cells compared with mock cells (Figure 2F–2H).

Schwann-like cell differentiation is involved in CXCR5 induced PNI in SACC cells

Schwann-like cell differentiation promoted migration and invasion of tumor cells [29]. Hence, we analyzed hallmarks of Schwann cell in CXCR5-induced SACC cells during PNI. Here, we found that knockdown or

Table 1. Relation of CXCR5 expression with clinicopathological parameters in 158 cases of SACC.

Clinicopathological parameters		cases	CXCR5 expression				*p* value
			–	+	++	+++	
		158	30	49	51	28	
Ages (years)	<50	73	12	27	23	11	0.642
	≥50	85	18	22	28	17	
Sex	Male	85	20	26	27	12	0.104
	Female	73	10	23	24	16	
Complaint (months)	<12	83	16	31	23	13	0.202
	≥12	75	14	18	28	15	
Site	Minor salivary gland	108	19	27	41	21	0.038
	Major salivary gland	50	11	22	10	7	
Tumor diameter (cm)	≤1	24	8	5	7	4	0.612
	1~2	45	9	13	13	10	
	≥2	89	13	31	31	14	
Clinical stage	I+II	70	24	13	24	9	0.017
	III+IV	88	6	36	27	19	
Histological subtype	Cribriform	72	13	28	27	4	0.008
	Tubular	49	12	12	18	7	
	Solid	37	5	9	6	17	
Involvement of surgical margin	Affect	48	6	12	19	11	0.04
	free	110	24	37	32	17	
Local regional recurrence	Positive	41	5	11	10	15	0.008
	Negative	117	25	38	41	13	
Distant metastasis	Positive	46	7	6	19	14	0.001
	Negative	112	23	43	32	14	

blockade of CXCR5 brought about a considerable downregulation of Schwann cell hallmarks, including S100A4, p75NTR, GFAP in SACC-LM cells compared with the control group (Figure 3A), whereas overexpression of CXCR5 induced upregulation of S100A4, p75NTR, GFAP (Figure 3B). Moreover, SACC cells underwent the transformation from an elongated, invasive, spindle-like fibroblastic cellular morphology to epithelial plasticity with cobblestone-like appearance and little branching after CXCR5 silence or blockade in SACC-LM cells (Figure 3C).

CXCR5 promotes the expression of Schwann cell markers by inhibiting miR-187

To determine the downstream miRNAs of CXCR5, SACC-LM cells were transfected with control siRNA or si-CXCR5 and microarray was performed to screen differentially expressed miRNAs. 8 differentially expressed miRNAs showed in Figure 3D were selected to validate by qPCR (Figure 3E) and miR-187 was the one with most dynamic expression. Based on the result, we investigated the effect of CXCR5 overexpressing on miR-187 and observed a remarkable downregulated trend of miR-187 (Figure 3F), thus we selected miR-187 for further investigation.

Next, we conducted RNA FISH assay using paraffin-embedded tissue samples, and results validated the downregulation of miR-187 in SACC tissues compared with NSG. In addition, miR-187 level presented a downward trend at nerve invasion frontier (Figure 4A). Thereafter, we predicted whether miR-187 had the potential to interact with Schwann cell markers via the bioinformatic tool starBase, and identified a putative binding site for miR-187 in the S100A4 sequence. Thus, we reasoned that CXCR5 manipulated PNI of SACC through repressing miR-187 to disinhibit S100A4. The binding sites on miR-187 and S100A4 3′UTR were presented in Figure 4B. Luciferase reporter assay

Table 2. Cox multivariate regression analysis of overall survival in SACC patients.

	B	SE	Wald	df	Sig.	Exp (B)	95.0% CI for Exp (B)	
							Lower	Upper
Clinical stage	0.749	0.280	7.140	1	0.008	2.115	1.221	3.663
Involvement of surgical margin	0.384	0.262	2.161	1	0.142	1.469	0.880	2.452
Local regional recurrence	0.892	0.292	9.357	1	0.002	2.440	1.378	4.320
PNI	0.728	0.254	8.212	1	0.004	2.070	1.259	3.405
Distant metastasis	0.884	0.254	12.085	1	0.001	2.421	1.471	3.985
CXCR5 expression	0.407	0.135	9.027	1	0.003	1.502	1.152	1.959

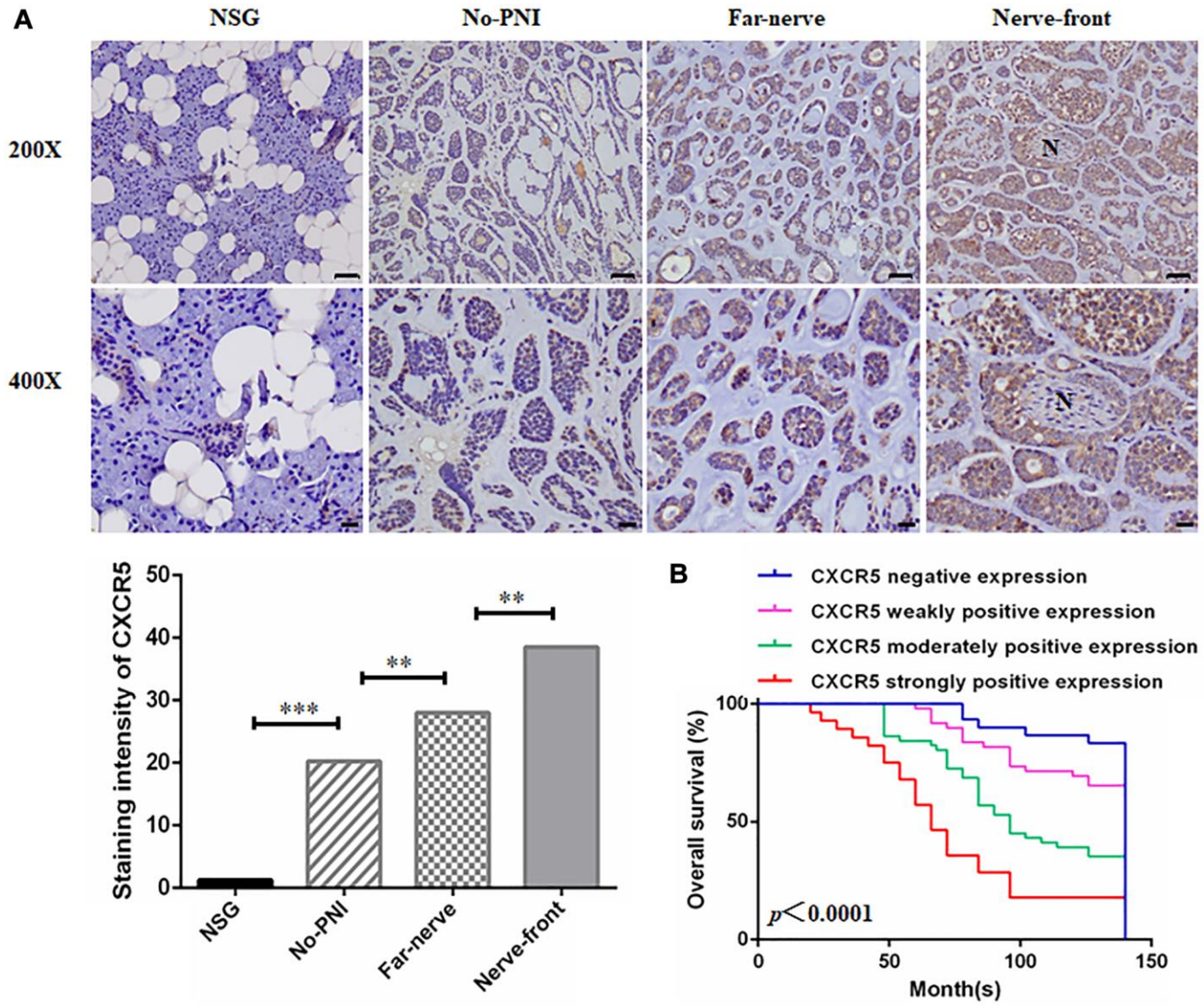

Figure 1. Clinical significance of CXCR5 expression in SACC patients. (**A**) Immunohistochemical staining of CXCR5 in normal salivary gland (NSG), SACC without PNI (No-PNI), far away from nerve of SACC with PNI (Far-nerve), nerve invasion front of SACC with PNI (Nerve-front). 'N' represented nerve. (Bar: upper, 50 μm; lower, 20 μm) ($^{**}p < 0.01$, $^{***}p < 0.001$). (**B**) Kaplan-Meier survival analysis on SACC patients with different expression status of CXCR5. The overall survival time for patients without or with low CXCR5 expression was longer than those with high CXCR5 expression (log-rank test, $p < 0.0001$).

Table 3. The expression of CXCR5 in normal salivary gland and SACC with different PNI status.

	Cases	NSG	No-PNI	Far-nerve	Nerve-front	*p* value
		(*n* = 20)	(*n* = 81)	(*n* = 77)	(*n* = 77)	
CXCR5	−	15	26	16	4	<0.0001
	+	5	34	25	15	
	++	0	16	21	35	
	+++	0	5	15	23	
	p value	0.0001	0.005	0.001		

NOTE: NSG, normal salivary gland group.

No-PNI, SACC without PNI group.

Far-nerve, far away from nerve of SACC with PNI group.

Nerve-front, nerve invasion front of SACC with PNI group.

showed that overexpressing miR-187 provoked efficient quenching the luciferase activity in S100A4 WT, but not notable difference in the S100A4 Mut (Figure 4C). QPCR analysis showed that the reduction of Schwann cell hallmarks mediated by CXCR5 silence could be partially relieved by miR-187 inhibitor (Figure 4D).

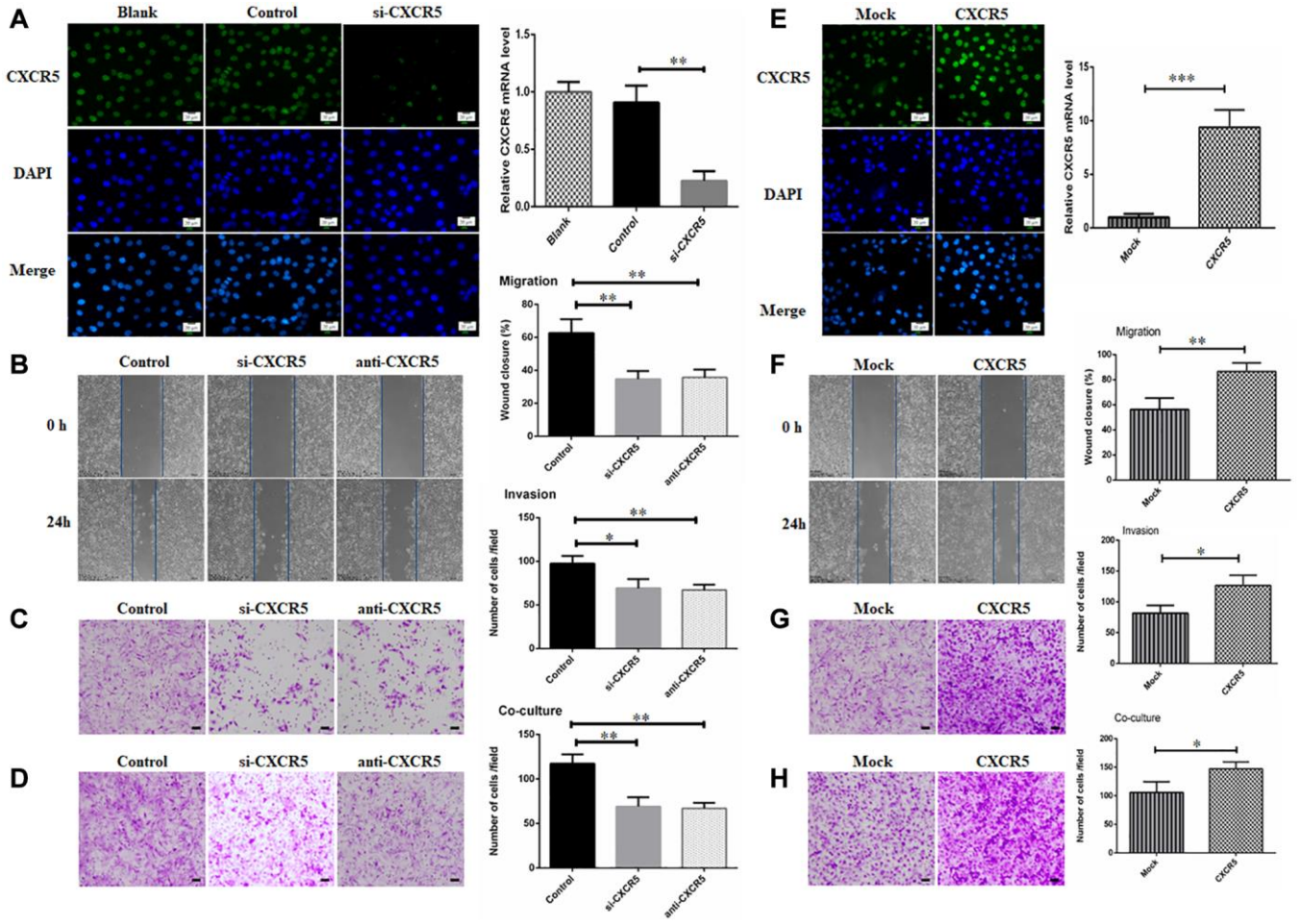

Figure 2. Silencing CXCR5 attenuates migration, invasion and PNI in SACC cells. (**A**) Immunofluorescence and qRT-PCR analysis showed that CXCR5 expression was dramatically inhibited by siRNA treatment. (**B**–**D**) CXCR5 silence with siRNA or CXCR5 blockade with anti-CXCR5 antibody impeded migration, invasion and PNI of SACC-LM cells, (Bar: 100 μm). (**E**) Immunofluorescence and qRT-PCR analysis showed that CXCR5 level was significantly increased by CXCR5-overexpressing plasmid. (**F**–**H**) CXCR5 overexpression enhanced migration, invasion and PNI capacity of SACC-LM cells, (Bar: 100 μm) ($^{*}p < 0.05$, $^{**}p < 0.01$, $^{***}p < 0.001$).

Those findings supported that miR-187 targeted and inhibited S100A4 activity in a direct binding manner. Further, inhibitory migratory, invasive and PNI ability in SACC-LM cells mediated by CXCR5 silence or miR-187 overexpression could be reversed by S100A4 overexpression (Figure 4E–4F).

Inhibition of CXCR5 suppresses PNI in SACC xenograft model

To further validate our findings, *in vivo* PNI model was conducted as described in methods. The results displayed that compared with saline group, the mice in anti-CXCR5 antibody group underwent less contracture and dysfunction of hindlimb paw, which was intervened by sciatic nerve. Xenografted tumors were excised for HE staining, and the results showed the incidence of PNI in saline group and anti-CXCR5 antibody group was 62.5% (5/8) and 12.5% (1/8), respectively (Figure 5A). The incidence of PNI was lower in anti-CXCR5 antibody group compared with saline group. Besides, the results of qRT-PCR (Figure 5B) and immunohistochemistry analysis (Figure 5C) showed that the expression of S100A4, p75NTR and GFAP was higher in anti-CXCR5 antibody group than that in saline group, besides, it was significantly increased at nerve invasion frontier in PNI group compared with tumors far away from nerve.

CXCR5 expression intrinsically connects with the level of Schwann cell markers in SACC specimens

Schwann cell related markers, including S100A4, p75NTR, GFAP were also examined by immunohistochemistry staining in 158 SACC specimens and 20 normal salivary glands (Figure 6A, Supplementary Figure 1). The associations between CXCR5 and Schwann cell hallmarks, including S100A4, p75NTR, GFAP at nerve invasion frontier of PNI groups in SACC were assessed. The results showed that

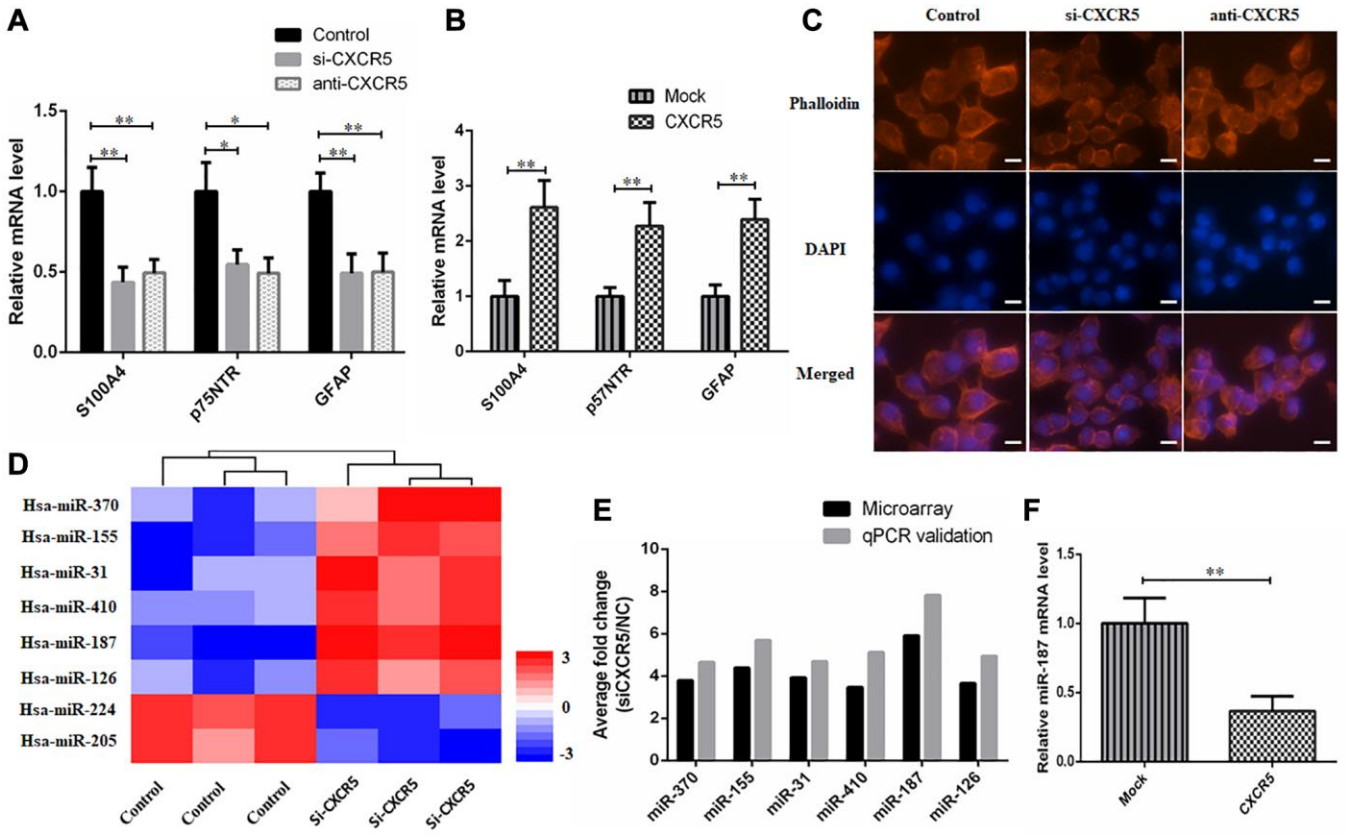

Figure 3. Schwann-like cell differentiation is involved in CXCR5 induced PNI in SACC cells. (**A**) CXCR5 silence with siRNA or CXCR5 blockade with anti-CXCR5 antibody downregulated the expression of Schwann cell markers, including S100A4, p75NTR, GFAP by qRT-PCR analyses. (**B**) CXCR5 overexpression upregulated the expression of S100A4, p75NTR, GFAP in SACC-LM cells. (**C**) CXCR5 silence with siRNA or CXCR5 blockade with anti-CXCR5 antibody resulted in the transformation of SACC-LM cells from spindle-like fibroblastic cellular morphology to epithelial plasticity with little pseudopodia, (Bar: 50 μm). (**D**) The heatmap of 8 differentially expressed miRNAs in SACC-LM cells transfected with control or si-CXCR5 on a scale from blue (low) to red (high). 'Blue' represents low expression, and 'red' represents high expression. (**E**) The microarray data of 8 differentially expressed miRNAs in the si-CXCR5 and control SACC-LM cells was confirmed by qRT-PCR. For qRT-PCR, U6 was used to normalize the Ct values. (**F**) CXCR5 overexpression upregulated the expression of miR-187 in SACC-LM cells, ($^{*}p < 0.05$, $^{**}p < 0.01$).

CXCR5 expression was positively correlated with the expression of S100A4 ($p < 0.0001$, $\gamma = 0.5489$), p75NTR ($p < 0.0001$, $\gamma = 0.3838$) and GFAP ($p < 0.0001$, $\gamma = 0.4037$) (Figure 6B).

DISCUSSION

PNI not only brings about dysfunction, but also causes the recurrence and metastasis in multiple malignant neoplasm, including head and neck [3, 9], pancreatic [35], prostate [10], colorectal [36], gastric [37], breast [8] cancer, and so on. In the present study, we found that CXCR5 was highly expressed in SACC tissue compared with normal salivary gland, and CXCR5 expression was significantly correlated with tumor site, clinical stage, histological subtype, involvement of surgical margin, local regional recurrence and distant metastasis. To our knowledge, this is the first study to confirm the possible clinical relevance of CXCR5 to SACC patients. To explore the relationship between CXCR5 and PNI, CXCR5 expression in different PNI status was also analyzed, and the results showed that CXCR5 expression at nerve invasion frontier was higher than far away from nerve site in SACC specimens. To verify above findings, we extended our research *in vitro*. The results showed that the migration

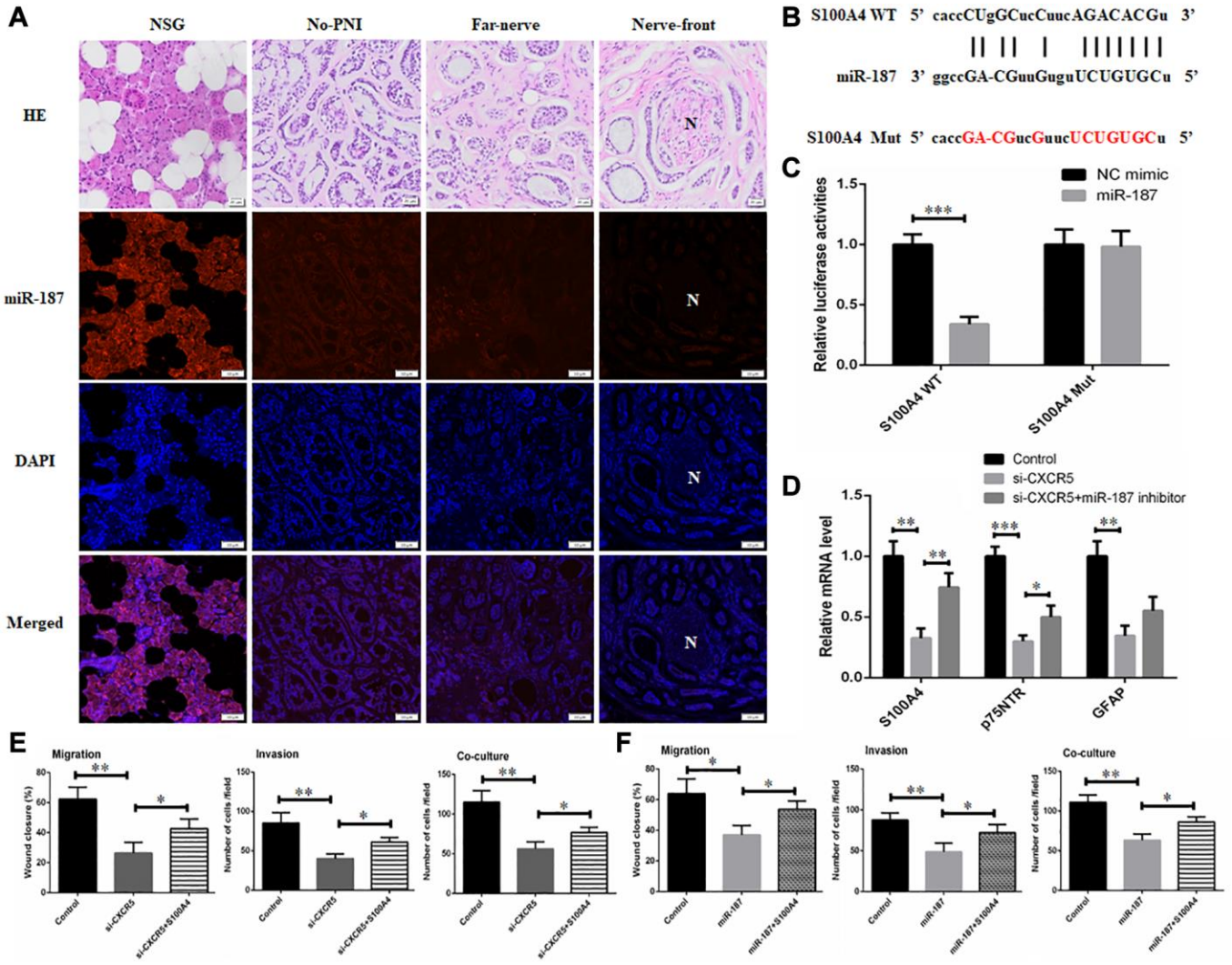

Figure 4. CXCR5 promotes the expression of Schwann cell markers by inhibiting miR-187. (**A**) An RNA-FISH assay was conducted to determine the level of miR-187 in normal salivary gland (NSG), SACC without PNI (No-PNI), far away from nerve of SACC with PNI (Far-nerve), nerve invasion front of SACC with PNI (Nerve-front). 'N' represented nerve, (Bar: 50 μm). (**B**) The binding sites on S100A4 3'UTR for miR-187 and the mutant sites. (**C**) Luciferase reporter analysis was carried out to determine the interaction of miR-187 with S100A4. (**D**) qRT-PCR analysis showed that reduced expression of Schwann cell hallmarks mediated by CXCR5 silence could be partially reversed by miR-187 inhibitor. (**E**) Inhibitory migratory, invasive and PNI ability in SACC-LM cells mediated by CXCR5 silence could be reversed by S100A4 overexpression. (**F**) Repressive migratory, invasive and PNI ability in SACC-LM cells induced miR-187 overexpression was alleviated by S100A4 overexpression, ($^{*}p < 0.05$, $^{**}p < 0.01$).

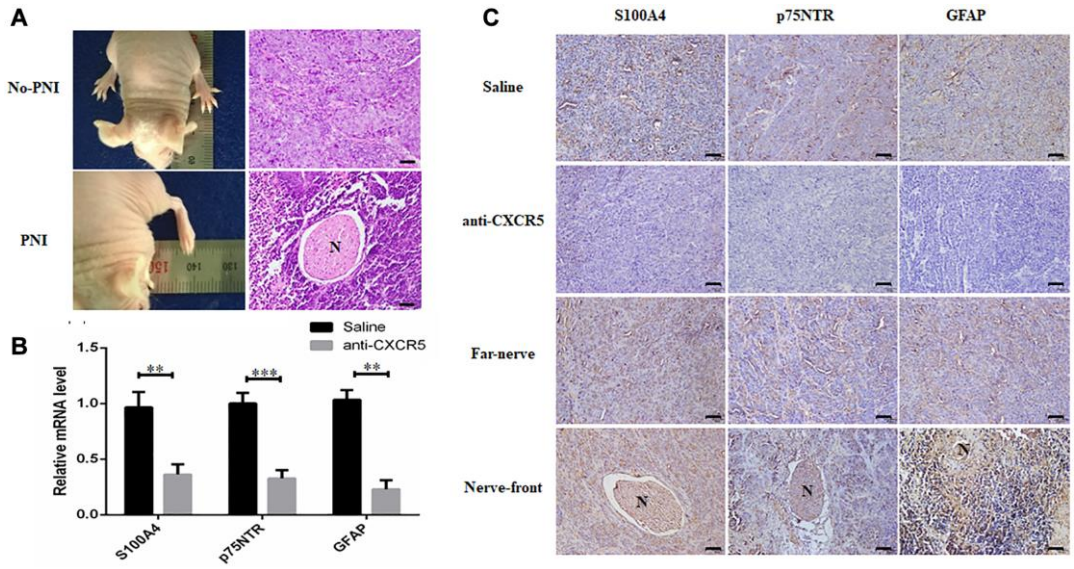

Figure 5. Inhibition of CXCR5 suppresses PNI in SACC xenograft model. (**A**) Representative images on hindlimb function of the mouse and HE staining were presented. (**B**) qRT-PCR analysis showed that anti-CXCR5 antibody group mice showed reduced expression of S100A4, p75NTR and GFAP compared with saline group mice. (**C**) Immunohistochemical staining showed that anti-CXCR5 antibody group mice showed reduced expression of S100A4, p75NTR and GFAP compared with saline group mice. The expression of S100A4, p75NTR, GFAP was higher at nerve invasion frontier than that in tumors far away from nerve in PNI groups, 'N' represented nerve, (Bar: 50 μm) ($^{**}p < 0.01$, $^{***}p < 0.001$).

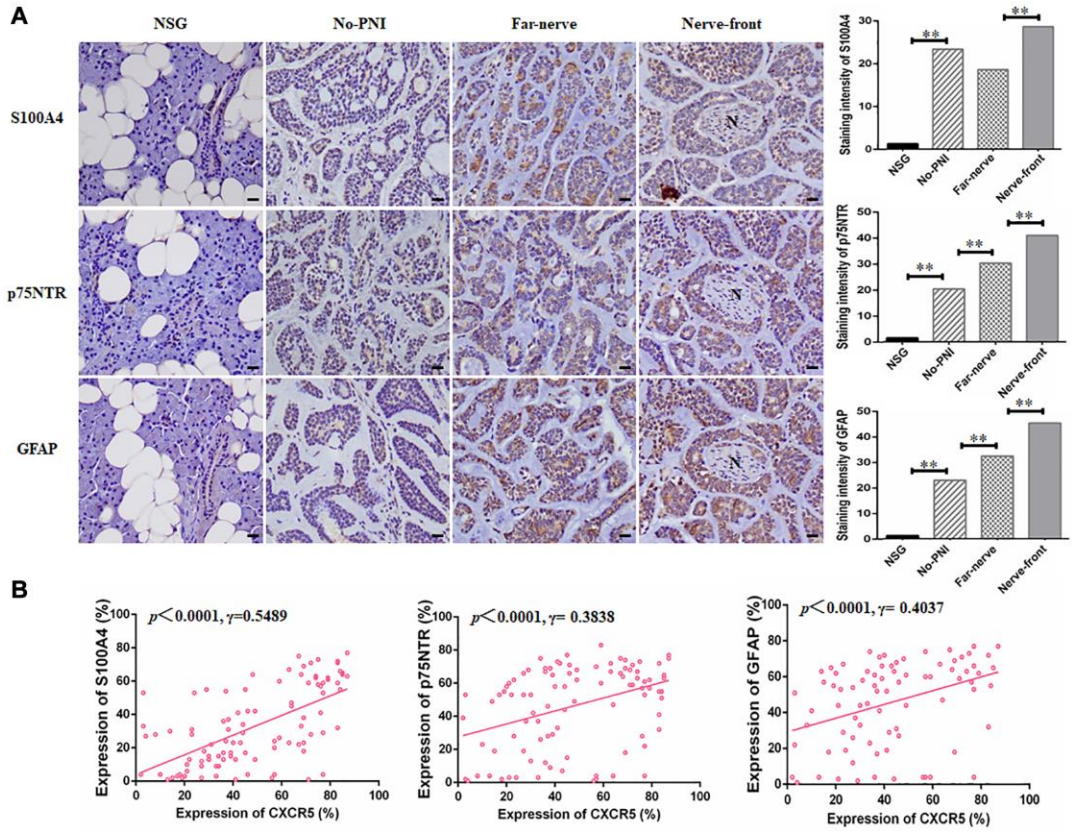

Figure 6. CXCR5 expression intrinsically connects with the level of Schwann cell markers in SACC specimens. (**A**) Immunohistochemical staining of Schwann cell markers, including S100A4, p75NTR and GFAP in normal salivary gland (NSG), SACC without PNI (No-PNI), far away nerve of SACC with PNI (Far-nerve), nerve invasion front of SACC with PNI (Nerve-front). 'N' represented nerve, (Bar: 20 μm). (**B**) Correlation of CXCR5 with Schwann cell markers at nerve invasion frontier of SACC patients. CXCR5 expression was positively correlated with the expression of S100A4, p75NTR and GFAP at nerve invasion frontier of SACC ($^{**}p < 0.01$).

and invasion and PNI of SACC cells could be inhibited by CXCR5 silence with siRNA or CXCR5 blockade with anti-CXCR5 antibody.

And these results were in accordance with the previous studies, which revealed that CXCR5 participated in the progression and poor prognosis in many types of cancers. For example, Li et al. confirmed that CXCR5 was significantly elevated and associated with the poor prognosis of HCC patients [38]. Singh et al. noted that CXCR5 accelerated malignant progression of lung cancer, and inhibition of CXCR5 may provide a new treatment strategy for lung cancer [39]. Rubenstein et al. identified that CXCR5 was promised to be a new target for the detection and treatment of lymphoma [40]. Qi et al. demonstrated that CXCR5 played a pivotal role in the growth, migration and invasion of colon cancer cell through PI3K/AKT pathway [16]. Singh et al. verified that CXCR5 mediated prostate cancer cell proliferation and invasion through the activation of Src, FAK, JNK and ERK1/2 signaling [17, 41]. Biswas et al. reported that CXCR5 induced invasion and metastasis through the activation of Src kinase signaling pathway in breast cancer [42].

Enhanced Schwann-like cell differentiation companied with cytoskeleton rearrangement and the pseudopodia formation of tumor cells is a crucial prerequisite for PNI [29, 43–45], by which tumor cells acquire fibroblast like morphology and mesenchymal traits to invade and metastasize. In this study, the elevated CXCR5 level was constantly accompanied by upregulated expression of S100A4, p75NTR and GFAP, which had been characterized as Schwann cell hallmarks [21, 46] at nerve invasion frontier. Decreased CXCR5 inhibited the expression of S100A4, p75NTR and GFAP and promoted transformation of SACC cells from spindle-like fibroblastic cellular morphology to epithelial plasticity with little pseudopodia. These revealed that Schwann-like cell differentiation might occur and CXCR5 might involve in the process of Schwann-like cell differentiation in PNI of SACC cells.

Dysregulation of miRNAs, which negatively orchestrate the expression of their target gene by binding to complementary 3′-UTR sequences of target mRNA, is known as an important mechanism contributing to PNI of tumors. In our present study, to further explore the role of miRNA in CXCR5 induced PNI of SACC, miRNA array analysis and potential target relationship prediction by Targetscan were performed. We found that miR-187, which harbored S100A4 binding sites, was the most increased miRNA after CXCR5 loss. Furthermore, we illustrated that miR-187 was markedly downregulated at the nerve invasion frontier by FISH. Dual luciferase reporter assays and rescue experiments confirmed CXCR5-dependent regulation of PNI was achieved by miR-187 silence to derepress S100A4 expression. The inhibitory effect of migration, invasion and PNI by CXCR5 knockdown or miR-187 overexpression could be reversed through S100A4 overexpression.

Taken together, the present study demonstrated that CXCR5 triggered the differentiation of tumor cells into Schwann-like cells through repressing miR-187 to disinhibit S100A4, thus facilitating PNI of SACC.

Abbreviations

PNI: Perineural invasion; SACC: Salivary adenoid cystic carcinoma; miR-187: MicroRNA-187; GPCR: G-protein coupled receptors; RISC: RNA-induced silencing complex; S100A4: S100 calcium binding protein A4; p75NTR: P75 neurotrophin receptor; GFAP: Glial fibrillary acidic protein; IHC: Immunohistochemistry; DMEM: Dulbecco's Modified Eagle's Medium; FBS: Fetal bovine serum; DAPI: Diamidino-2-phenylindole; qRT-PCR: Quantitative real-time PCR.

AUTHOR CONTRIBUTIONS

Mei Zhang: Data curation; Formal analysis; Investigation; Methodology. Visualization; Writing-original draft. Jia-shun Wu, Hong-chun Xian, Bing-jun Chen, Hao-fan Wang, Xiang-hua Yu, Xin Pang, Li Dai and Jian Jiang: Investigation; Methodology; Visualization. Xin-hua Liang and Ya-ling Tang: Conceptualization; Funding acquisition; Review of the manuscript.

ACKNOWLEDGMENTS

This work was supported by National Natural Science Foundation of China grants (Nos. 81972542 and 82073000) and Science and Technology of Sichuan Province (No. 2020YFS0171 and 2020JDRC0018).

CONFLICTS OF INTEREST

The authors declare no conflicts of interest related to this study.

REFERENCES

1. Ord RA, Ghazali N. Margin Analysis: Malignant Salivary Gland Neoplasms of the Head and Neck. Oral Maxillofac Surg Clin North Am. 2017; 29:315–24. https://doi.org/10.1016/j.coms.2017.03.008 PMID:28551337

2. Alfieri S, Granata R, Bergamini C, Resteghini C, Bossi P, Licitra LF, Locati LD. Systemic therapy in metastatic salivary gland carcinomas: A pathology-driven paradigm? Oral Oncol. 2017; 66:58–63. https://doi.org/10.1016/j.oraloncology.2016.12.016 PMID:28249649

3. Liebig C, Ayala G, Wilks JA, Berger DH, Albo D. Perineural invasion in cancer: a review of the literature. Cancer. 2009; 115:3379–91. https://doi.org/10.1002/cncr.24396 PMID:19484787

4. Gündüz AK, Yeşiltaş YS, Shields CL. Overview of benign and malignant lacrimal gland tumors. Curr Opin Ophthalmol. 2018; 29:458–68. https://doi.org/10.1097/ICU.0000000000000515 PMID:30028745

5. Bradley PJ. Adenoid cystic carcinoma evaluation and management: progress with optimism! Curr Opin Otolaryngol Head Neck Surg. 2017; 25:147–53. https://doi.org/10.1097/MOO.0000000000000347 PMID:28106659

6. Coca-Pelaz A, Rodrigo JP, Bradley PJ, Vander Poorten V, Triantafyllou A, Hunt JL, Strojan P, Rinaldo A, Haigentz M Jr, Takes RP, Mondin V, Teymoortash A, Thompson LD, Ferlito A. Adenoid cystic carcinoma of the head and neck--An update. Oral Oncol. 2015; 51:652–61. https://doi.org/10.1016/j.oraloncology.2015.04.005 PMID:25943783

7. Laurie SA, Ho AL, Fury MG, Sherman E, Pfister DG. Systemic therapy in the management of metastatic or locally recurrent adenoid cystic carcinoma of the salivary glands: a systematic review. Lancet Oncol. 2011; 12:815–24. https://doi.org/10.1016/S1470-2045(10)70245-X PMID:21147032

8. Zheng SC, Zhang YR, Luo SY, Zhang LP. [The effect of GDNF on matrix-degrading and cell-adhesion during perineural invasion of salivary adenoid cystic carcinoma]. Shanghai Kou Qiang Yi Xue. 2016; 25:212–16. PMID:27329888

9. Pour PM, Bell RH, Batra SK. Neural invasion in the staging of pancreatic cancer. Pancreas. 2003; 26:322–25. https://doi.org/10.1097/00006676-200305000-00002 PMID:12717262

10. Liebig C, Ayala G, Wilks J, Verstovsek G, Liu H, Agarwal N, Berger DH, Albo D. Perineural invasion is an independent predictor of outcome in colorectal cancer. J Clin Oncol. 2009; 27:5131–37. https://doi.org/10.1200/JCO.2009.22.4949 PMID:19738119

11. Widney DP, Gui D, Popoviciu LM, Said JW, Breen EC, Huang X, Kitchen CM, Alcantar JM, Smith JB, Detels R, Martínez-Maza O. Expression and Function of the Chemokine, CXCL13, and Its Receptor, CXCR5, in Aids-Associated Non-Hodgkin's Lymphoma. AIDS Res Treat. 2010; 2010:164586. https://doi.org/10.1155/2010/164586 PMID:21490903

12. Bagaeva LV, Rao P, Powers JM, Segal BM. CXC chemokine ligand 13 plays a role in experimental autoimmune encephalomyelitis. J Immunol. 2006; 176:7676–85. https://doi.org/10.4049/jimmunol.176.12.7676 PMID:16751415

13. Hussain M, Adah D, Tariq M, Lu Y, Zhang J, Liu J. CXCL13/CXCR5 signaling axis in cancer. Life Sci. 2019; 227:175–86. https://doi.org/10.1016/j.lfs.2019.04.053 PMID:31026453

14. Zheng Z, Cai Y, Chen H, Chen Z, Zhu D, Zhong Q, Xie W. CXCL13/CXCR5 Axis Predicts Poor Prognosis and Promotes Progression Through PI3K/AKT/mTOR Pathway in Clear Cell Renal Cell Carcinoma. Front Oncol. 2019; 8:682. https://doi.org/10.3389/fonc.2018.00682 PMID:30723697

15. Garg R, Blando JM, Perez CJ, Abba MC, Benavides F, Kazanietz MG. Protein Kinase C Epsilon Cooperates with PTEN Loss for Prostate Tumorigenesis through the CXCL13-CXCR5 Pathway. Cell Rep. 2017; 19:375–88. https://doi.org/10.1016/j.celrep.2017.03.042 PMID:28402859

16. Qi XW, Xia SH, Yin Y, Jin LF, Pu Y, Hua D, Wu HR. Expression features of CXCR5 and its ligand, CXCL13 associated with poor prognosis of advanced colorectal cancer. Eur Rev Med Pharmacol Sci. 2014; 18:1916–24. PMID:25010623

17. Singh S, Singh R, Singh UP, Rai SN, Novakovic KR, Chung LW, Didier PJ, Grizzle WE, Lillard JW Jr. Clinical and biological significance of CXCR5 expressed by prostate cancer specimens and cell lines. Int J Cancer. 2009; 125:2288–95. https://doi.org/10.1002/ijc.24574 PMID:19610059

18. Bartel DP. MicroRNAs: target recognition and regulatory functions. Cell. 2009; 136:215–33. https://doi.org/10.1016/j.cell.2009.01.002 PMID:19167326

19. Filipowicz W, Bhattacharyya SN, Sonenberg N. Mechanisms of post-transcriptional regulation by

microRNAs: are the answers in sight? Nat Rev Genet. 2008; 9:102–14.
https://doi.org/10.1038/nrg2290
PMID:18197166

20. Ambs S, Prueitt RL, Yi M, Hudson RS, Howe TM, Petrocca F, Wallace TA, Liu CG, Volinia S, Calin GA, Yfantis HG, Stephens RM, Croce CM. Genomic profiling of microRNA and messenger RNA reveals deregulated microRNA expression in prostate cancer. Cancer Res. 2008; 68:6162–70.
https://doi.org/10.1158/0008-5472.CAN-08-0144
PMID:18676839

21. Ziegler L, Grigoryan S, Yang IH, Thakor NV, Goldstein RS. Efficient generation of schwann cells from human embryonic stem cell-derived neurospheres. Stem Cell Rev Rep. 2011; 7:394–403.
https://doi.org/10.1007/s12015-010-9198-2
PMID:21052870

22. Ramli K, Aminath Gasim I, Ahmad AA, Hassan S, Law ZK, Tan GC, Baharuddin A, Naicker AS, Htwe O, Mohammed Haflah NH, Idrus RBH, Abdullah S, Ng MH. Human bone marrow-derived MSCs spontaneously express specific Schwann cell markers. Cell Biol Int. 2019; 43:233–52.
https://doi.org/10.1002/cbin.11067
PMID:30362196

23. Carlson JA, Dickersin GR, Sober AJ, Barnhill RL. Desmoplastic neurotropic melanoma. A clinicopathologic analysis of 28 cases. Cancer. 1995; 75:478–94.
https://doi.org/10.1002/1097-0142(19950115)75:2<478::aid-cncr2820750211>3.0.co;2-o
PMID:7812919

24. Kwon SY, Bae YK, Gu MJ, Choi JE, Kang SH, Lee SJ, Kim A, Jung HR, Kang SH, Oh HK, Park JY. Neuroendocrine differentiation correlates with hormone receptor expression and decreased survival in patients with invasive breast carcinoma. Histopathology. 2014; 64:647–59.
https://doi.org/10.1111/his.12306
PMID:24117859

25. Park K, Chen Z, MacDonald TY, Siddiqui J, Ye H, Erbersdobler A, Shevchuk MM, Robinson BD, Sanda MG, Chinnaiyan AM, Beltran H, Rubin MA, Mosquera JM. Prostate cancer with Paneth cell-like neuroendocrine differentiation has recognizable histomorphology and harbors AURKA gene amplification. Hum Pathol. 2014; 45:2136–43.
https://doi.org/10.1016/j.humpath.2014.06.008
PMID:25128228

26. Harada K, Sato Y, Ikeda H, Isse K, Ozaki S, Enomae M, Ohama K, Katayanagi K, Kurumaya H, Matsui A, Nakanuma Y. Epithelial-mesenchymal transition induced by biliary innate immunity contributes to the sclerosing cholangiopathy of biliary atresia. J Pathol. 2009; 217:654–64.
https://doi.org/10.1002/path.2488
PMID:19116990

27. Demir IE, Boldis A, Pfitzinger PL, Teller S, Brunner E, Klose N, Kehl T, Maak M, Lesina M, Laschinger M, Janssen KP, Algül H, Friess H, Ceyhan GO. Investigation of Schwann cells at neoplastic cell sites before the onset of cancer invasion. J Natl Cancer Inst. 2014; 106:dju184.
https://doi.org/10.1093/jnci/dju184
PMID:25106646

28. Deborde S, Wong RJ. How Schwann cells facilitate cancer progression in nerves. Cell Mol Life Sci. 2017; 74:4405–20.
https://doi.org/10.1007/s00018-017-2578-x
PMID:28631007

29. Shan C, Wei J, Hou R, Wu B, Yang Z, Wang L, Lei D, Yang X. Schwann cells promote EMT and the Schwann-like differentiation of salivary adenoid cystic carcinoma cells via the BDNF/TrkB axis. Oncol Rep. 2016; 35:427–35.
https://doi.org/10.3892/or.2015.4366
PMID:26530352

30. da Cruz Perez DE, de Abreu Alves F, Nobuko Nishimoto I, de Almeida OP, Kowalski LP. Prognostic factors in head and neck adenoid cystic carcinoma. Oral Oncol. 2006; 42:139–46.
https://doi.org/10.1016/j.oraloncology.2005.06.024
PMID:16249115

31. He S, He S, Chen CH, Deborde S, Bakst RL, Chernichenko N, McNamara WF, Lee SY, Barajas F, Yu Z, Al-Ahmadie HA, Wong RJ. The chemokine (CCL2-CCR2) signaling axis mediates perineural invasion. Mol Cancer Res. 2015; 13:380–90.
https://doi.org/10.1158/1541-7786.MCR-14-0303
PMID:25312961

32. Lee TL, Chiu PH, Li WY, Yang MH, Wei PY, Chu PY, Wang YF, Tai SK. Nerve-tumour interaction enhances the aggressiveness of oral squamous cell carcinoma. Clin Otolaryngol. 2019; 44:1087–95.
https://doi.org/10.1111/coa.13452
PMID:31574203

33. Widney DP, Olafsen T, Wu AM, Kitchen CM, Said JW, Smith JB, Peña G, Magpantay LI, Penichet ML, Martinez-Maza O. Levels of murine, but not human, CXCL13 are greatly elevated in NOD-SCID mice bearing the AIDS-associated Burkitt lymphoma cell line, 2F7. PLoS One. 2013; 8:e72414.
https://doi.org/10.1371/journal.pone.0072414
PMID:23936541

34. Ikeda T, Nishita M, Hoshi K, Honda T, Kakeji Y, Minami Y. Mesenchymal stem cell-derived CXCL16 promotes progression of gastric cancer cells by STAT3-mediated expression of Ror1. Cancer Sci. 2020; 111:1254–65. https://doi.org/10.1111/cas.14339 PMID:32012403

35. Feng FY, Qian Y, Stenmark MH, Halverson S, Blas K, Vance S, Sandler HM, Hamstra DA. Perineural invasion predicts increased recurrence, metastasis, and death from prostate cancer following treatment with dose-escalated radiation therapy. Int J Radiat Oncol Biol Phys. 2011; 81:e361–67. https://doi.org/10.1016/j.ijrobp.2011.04.048 PMID:21820250

36. Deng J, You Q, Gao Y, Yu Q, Zhao P, Zheng Y, Fang W, Xu N, Teng L. Prognostic value of perineural invasion in gastric cancer: a systematic review and meta-analysis. PLoS One. 2014; 9:e88907. https://doi.org/10.1371/journal.pone.0088907 PMID:24586437

37. Figueira RC, Gomes LR, Neto JS, Silva FC, Silva ID, Sogayar MC. Correlation between MMPs and their inhibitors in breast cancer tumor tissue specimens and in cell lines with different metastatic potential. BMC Cancer. 2009; 9:20. https://doi.org/10.1186/1471-2407-9-20 PMID:19144199

38. Li B, Su H, Cao J, Zhang L. CXCL13 rather than IL-31 is a potential indicator in patients with hepatocellular carcinoma. Cytokine. 2017; 89:91–97. https://doi.org/10.1016/j.cyto.2016.08.016 PMID:27663978

39. Singh R, Gupta P, Kloecker GH, Singh S, Lillard JW Jr. Expression and clinical significance of CXCR5/CXCL13 in human non-small cell lung carcinoma. Int J Oncol. 2014; 45:2232–40. https://doi.org/10.3892/ijo.2014.2688 PMID:25271023

40. Rubenstein JL, Wong VS, Kadoch C, Gao HX, Barajas R, Chen L, Josephson SA, Scott B, Douglas V, Maiti M, Kaplan LD, Treseler PA, Cha S, et al. CXCL13 plus interleukin 10 is highly specific for the diagnosis of CNS lymphoma. Blood. 2013; 121:4740–48. https://doi.org/10.1182/blood-2013-01-476333 PMID:23570798

41. El Haibi CP, Sharma PK, Singh R, Johnson PR, Suttles J, Singh S, Lillard JW Jr. PI3Kp110-, Src-, FAK-dependent and DOCK2-independent migration and invasion of CXCL13-stimulated prostate cancer cells. Mol Cancer. 2010; 9:85. https://doi.org/10.1186/1476-4598-9-85 PMID:20412587

42. Biswas S, Sengupta S, Roy Chowdhury S, Jana S, Mandal G, Mandal PK, Saha N, Malhotra V, Gupta A, Kuprash DV, Bhattacharyya A. CXCL13-CXCR5 co-expression regulates epithelial to mesenchymal transition of breast cancer cells during lymph node metastasis. Breast Cancer Res Treat. 2014; 143:265–76. https://doi.org/10.1007/s10549-013-2811-8 PMID:24337540

43. Iwamoto S, Odland PB, Piepkorn M, Bothwell M. Evidence that the p75 neurotrophin receptor mediates perineural spread of desmoplastic melanoma. J Am Acad Dermatol. 1996; 35:725–31. https://doi.org/10.1016/s0190-9622(96)90728-8 PMID:8912568

44. Luo XL, Sun MY, Lu CT, Zhou ZH. The role of Schwann cell differentiation in perineural invasion of adenoid cystic and mucoepidermoid carcinoma of the salivary glands. Int J Oral Maxillofac Surg. 2006; 35:733–39. https://doi.org/10.1016/j.ijom.2006.01.012 PMID:16513325

45. Chen W, Dong S, Zhou J, Sun M. Investigation of myoepithelial cell differentiation into Schwann-like cells in salivary adenoid cystic carcinoma associated with perineural invasion. Mol Med Rep. 2012; 6:755–59. https://doi.org/10.3892/mmr.2012.1003 PMID:22842649

46. Xie S, Lu F, Han J, Tao K, Wang H, Simental A, Hu D, Yang H. Efficient generation of functional Schwann cells from adipose-derived stem cells in defined conditions. Cell Cycle. 2017; 16:841–51. https://doi.org/10.1080/15384101.2017.1304328 PMID:28296571

SUPPLEMENTARY MATERIALS

Supplementary Figure

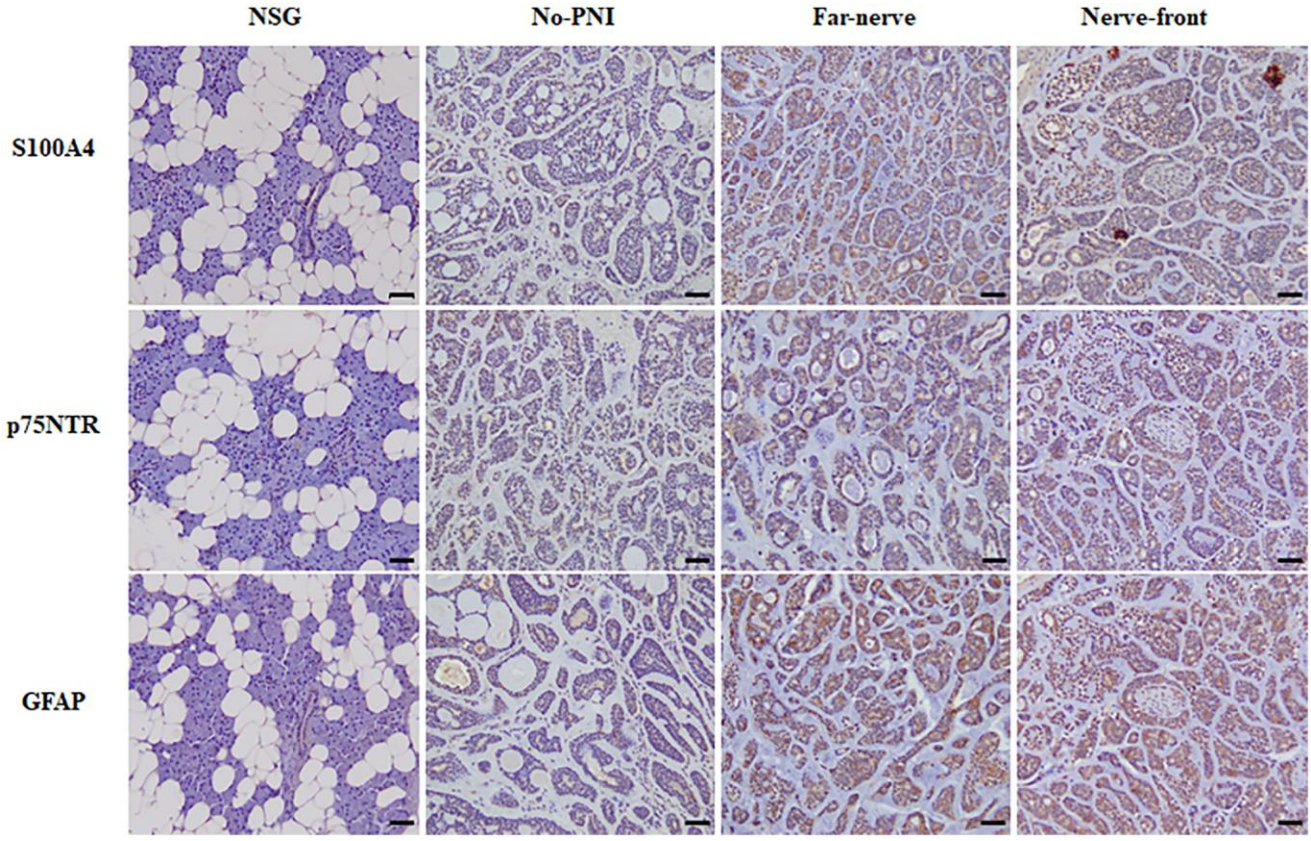

Supplementary Figure 1. Immunohistochemical staining of S100A4, p75NTR and GFAP in normal salivary gland (NSG), SACC without PNI (No-PNI), far away from nerve of SACC with PNI (Far-nerve), nerve invasion front of SACC with PNI (Nerve-front), (Bar: 50 μm).

Supplementary Table

Supplementary Table 1. The primer sequences of genes.

Gene	Primers (5'-3')
CXCR5-F	CGGCAGACACGCAGTTCCAC
CXCR5-R	ACGGCAAAGGGCAAGATGAAGAC
S100A4-F	GTACTCGGGCAAAGAGGGTG
S100A4-R	TTGTCCCTGTTGCTGTCCAA
P75NTR-F	CCTACGGCTACTACCAGGAT
P75NTR-R	TGGCCTCGTCGGAATACG
GFAP-F	CCGACAGCAGGTCCATGTG
GFAP-R	GTTGCTGGACGCCATTGC
GAPDH-F	CTTTGGTATCGTGGAAGGACTC
GAPDH-R	GTAGAGGCAGGGATGATGTTCT
Hsa-miR-370-F	CCAGGTCACGTCTCTGCAGTTAC
Hsa-miR-155-F	CGCGCGCTCCTACATATTAGCATTAAC
Hsa-miR-31-F	CCGTGCTATGCCAACATATTGCCAT
Hsa-miR-410-F	CGCGAATATAACACAGATGGCCTGT
Hsa-miR-187-F	CTCGTGTCTTGTGTTGCAGCC
Hsa-miR-126-F	CGCGCATTATTACTTTTGGTACGCG
Hsa-miR-224-F	GCGAAAATGGTGCCCTAGTGACTAC
Hsa-miR-205-F	CCGCGATTTCAGTGGAGTGAAGTTC